High optical performance of cyan-emissive $CsPbBr_3$ perovskite quantum dots embedded in molecular organogels

Marta Vallés-Pelarda, Andrés F. Gualdrón-Reyes, Carles Felip-León, César A. Angulo-Pachón, Said Agouram, Vicente Muñoz-Sanjosé, Juan F. Miravet, Francisco Galindo*, Iván Mora-Seró**

M. Vallés-Pelarda, Dr. A. F. Gualdrón-Reyes, Prof. I. Mora-Seró

Institute of Advanced Materials (INAM), University Jaume I. Av. de Vicent Sos Baynat, s/n 12006, Castelló de la Plana, Spain.

E-mail: sero@uji.es

Dr. C. Felip-León, Dr. C. A. Angulo-Pachón, Prof. Juan F. Miravet, Prof. Francisco Galindo

Department of Inorganic and Organic Chemistry, University Jaume I, Av. de Vicent Sos Baynat, s/n 12006, Castelló de la Plana, Spain.

E-mail: francisco.galindo@uji.es, miravet@uji.es

Dr. S. Agouram, Prof. V.Muñoz-Sanjosé

Department of Applied Physics and Electromagnetism, University of Valencia, 46100 Valencia, Spain.

Prof. I. Mora-Seró, Dr. S. Agouram, Prof. V. Muñoz-Sanjosé

Materials for Renewable Energy (MAER), Unitat Mixta d'Investigació UV-UJI

Keywords: perovskite quantum dots, organogels, blue emission, photoluminescence quantum yield

Abstract

Perovskite quantum dots (QDs) have fascinating optoelectronic properties, such as high photoluminescence quantum yield (PLQY) for a broad range of materials, and the possibility to obtain different band gaps with the same material or halide combinations. Nevertheless, blue-emissive materials generally present limited PLQY or color instability. Here, two molecular organogels, based on a derivative of an amino acid and succinic acid, were used to embed $CsPbBr_3$ quantum dots, obtaining green and blue emission. TEM and SAED measurements

were performed to confirm that there were no significant changes in the average size of the QDs and the crystal structure. A high near-unity PLQY was achieved for the blue emission. This contribution opens the door to a post-synthetic treatment for synthesizing blue-emissive PQDs with high optical performance, which can be attractive for optoelectronic applications.

1. Introduction

Perovskite quantum dots (PQDs) have been widely studied due to their exceptional properties, such as high photoluminescence with narrow emission peaks and high absorption coefficient. In addition, their band gap can be easily tuned by changing their chemical composition (different halides or mixed halides) or varying the morphology of the nanoparticles (NPs).[1–4] All of these properties make them suitable for many different applications: optoelectronic devices, lasers, scintillators, sensors. [5–10] Although the emission wavelength of these NPs can be tuned from UV to near IR, the achievement of a high photoluminescence quantum yield (PLQY) in blue emissive PQDs is still challenging. This is the case of $CsPbCl_3$ PQDs, whose PLQY is very low, the consequence of a high density of structural defects.[11] One strategy to increase the PLQY of these PQDs is by carrying out a mixture of halides (Br/Cl). However, these materials could show phase segregation and color instability.[12] Consequently, other approaches to optimize synthetic protocols for preparing PQDs with enhanced optical properties have been successfully studied.[13] In the case of $CsPbBr_3$ PQDs, the synthesis of blue-emissive nanoplatelets provides a PLQY ~70%,[1] while the preparation of sky-blue quasi-2D perovskites allows reaching a PLQY up to 88%.[10] Besides, by doping this kind of PQDs with neodymium, a PLQY up to 90% is achieved.[14] In the case of $CsPbCl_3$ PQDs, the post-treatment with $CdCl_2$ enables to obtain near-unity PLQY.[13]

Previous reports have incorporated NPs in a gel matrix, showing different effects such as an enhancement of the PL emission, a small redshift in the emission wavelength or even anion exchange reactions of PQDs that take place inside.[14–17] However, replacing the capping ligands of different NPs have shown some variations around 0.3 eV in the bandgap.[18,19] A recent work has reported a blueshift in the emission of $CsPbBr_3$ PQDs after a ligand exchange and this blueshift was explained by the reduction of particle size.[20] In addition, PQDs have been also embedded in some interesting matrices such as SiO_2,[21] poly(methylmethacrylate),[22] CaF_2 hierarchical nanospheres,[23] and so on, showing an efficient material encapsulation to improve long-term stability even in a polar ambient or moisture. However, the embedding process requires the mixture of PQDs with polar solvents in some cases, promoting the formation of agglomerates and deteriorating their photophysical properties due to the emergence of carrier traps.[24] Thus, it is essential to provide a potential matrix where not only the stability of PQDs can be extended, but also improves their intrinsic properties.

In this work, a mixture of $CsPbBr_3$ PQDs and organogelator molecules is presented, exhibiting a modification of their optical properties, specially a blueshift in the band gap and an enhancement of the PLQY. $CsPbBr_3$ PQDs embedded in the gel matrices show different emission wavelengths, green or blue, depending on the organogelator structure. The highest PLQY, near- unity, is achieved for blue emission, keeping around 80% of the initial value after 4 months. This improvement is associated with efficient surface passivation provided by the organogelator, Hx, covering the PQDs and reducing structural defects provided mainly by the loss of capping ligands. The combination of organic gels and PQDs can be useful to improve the photophysical properties of NPs, which can increase their interest in optoelectronics.

2. Results and discussion

Molecular organogelators studied in this work are the derivatives of an amino acid and succinic acid. This type of compounds forms fibrillar structures after a heating/cooling procedure, as described in the Experimental Section and also in **Figure S1**. The difference between these is the aliphatic chain arrangement of a radical; one is a linear hexyl radical (Hx) and the other is a cyclohexyl radical (Chx) (see **Figure 1a)**.[25] This small difference has shown to have a strong influence on the PQD properties after the gel formation. Comparing these organic molecules with the ligands surrounding the PQDs (oleic acid and oleylamine, OA and OLEA, respectively), they have similar functional groups. The gelator with the cyclohexyl moiety preserves the properties of the $CsPbBr_3$ PQDs, it emits green. However, when the chain is linear, it shows a blue emission. In **Figure 1b**, both gel matrices embedding PQDs are shown under UV light and the different behavior is observed. As mentioned before, the solutions need to be heated in order to obtain the different gels. For that reason, the effect of the temperature was first studied. A PQDs solution was heated following the procedure to form the gel and it was characterized by TEM (Figure S1). The formation of some big NPs is observed, increasing the average size by around 1 nm, which could be attributed to the Ostwald ripening process.[26,27] In addition, the effect on the PLQY was also analyzed. Although first measurements after the treatment of the NPs usually showed a decrease in the quantum yield, over the time, it was recovered almost completely.

Figure 1c shows the normalized PL spectra of the $CsPbBr_3$ PQDs colloidal solution and the PQDs embedded in both organogels. Taking as a reference the emission wavelength of the PQDs in solution at 507 nm, a small redshift of approximately 7 nm is observed for the Chx matrix (Chx-PQDs), while a blueshift of around 20 nm is observed in the Hx matrix (Hx-PQDs). The full width at half maximum (FWHM) of the PL peaks are 29 nm for the PQDs solution, 26

nm for the Hx-PQDs and 35 nm for the Chx-PQDs. As mentioned before, it has been reported the use of amino acids such as α-amino butyric acid after the synthesis of $CsPbBr_3$ PQDs, and the impact on their photophysical properties.[20] Because of the bi-functional structure of the α-amino butyric acid, it is proposed a ligand exchange process with conventional OA and OLEA, causing better surface passivation, and thereby the enhancement in the optical performances. This fact includes a blueshift in the PL peak, indication of the surface modification with a short-capping ligand, also mediating the decrease of PQDs size. In this context, we can suggest that Hx is promoting a surface passivation of $CsPbBr_3$ PQDs, obtaining a blueshift in their optical properties. Interestingly, the opposite effect is observed for Chx, which allows to infer that the surface coverage of PQDs is hindered. In order to explain this difference, it must be recalled that Hx and Chx self-associate in a very different manner, as it was demonstrated in the past: whereas the molecular architecture of Chx enables an efficient self-assembly and packing into fibres, Hx is less prone to self-associate. This indicates that Hx molecules could be more available to participate in the passivation process than Chx molecules.[25] Diverse heating temperatures were used, analyzing their effect on the Hx-PQDs emission. In **Table S1**, a comparison of the emission wavelengths with these temperatures is shown. In addition, a sample with low concentration of the Hx was prepared to observe the behavior of the PQDs when the gel is not completely formed, see **Figure S2**. It is observed that the blueshift is also produced in these conditions, indicating the gel formation is not the determining step for this blueshift.

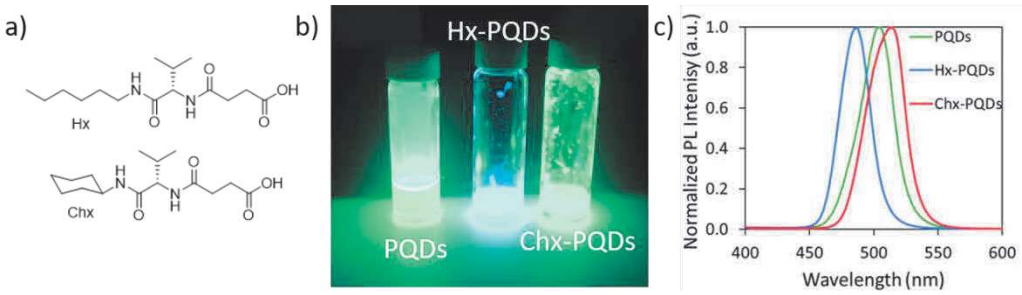

Figure 1. a) Chemical structure of the two different organogelators, Hx and Chx. b) Picture of the PQDs solution (left), Hx-PQDs (center) and Chx-PQDs (right) under UV light. c) Normalized PL spectra of the different samples: $CsPbBr_3$ PQDs solution (green), Hx matrix with $CsPbBr_3$ PQDs (blue) and Chx matrix with $CsPbBr_3$ PQDs (red).

Size, morphology and elemental composition of the Hx-PQDs and Chx-PQDs samples were analyzed by high-resolution transmission electron microscopy (HRTEM), selected area electron diffraction (SAED) and energy-dispersive X-ray spectroscopy (EDS). TEM images of PQDs colloidal solution is shown in **Figure 2a**. The chemical composition obtained from EDS measurements is shown in **Table S2**. From the TEM images in **Figure 2b-c**, an arrangement of PQDs following the fibers is observed for Hx-PQDs and Chx-PQDs samples. By estimating the particle size of the samples, we observed that the size of $CsPbBr_3$ PQDs is around 8.7 ± 2.5 nm, while Hx-PQDs show a slight decrease in the size, it is around 8.3 ± 1.9 nm. (see **Figure S3**). However, a clear difference in the particle size is seen for Chx-PQDs, around 14 ± 4 nm. The formation of smaller PQDs with a narrower size distribution in Hx-PQDs could be associated to the presence of the shorter chain ligand from the Hx. This fact induces a better uniformity and monodispersity of PQDs, which could slightly contribute to the blueshift in the PL.[20,28] Conversely, the bigger PQDs size and wider distribution obtained in presence of Chx are associated to the formation of agglomerates, generating lower uniformity in size and causing a redshift in the PL. These effects are also observed in the absorption measurements of the different samples, as shown in **Figure S4**.

Through SAED patterns shown in **Figure 2d-f**, interplanar spacings (*d*) were measured in order to determine the crystalline phase of the PQDs before and after embedding them in Hx and Chx matrices. Attending to the *d* values obtained from SAED rings, the corresponding diffraction planes found for PQDs, Hx-PQDs and Chx-PQDs are (020), (002), (040) and (242), from the orthorhombic phase (ICSD 231019). [29–31] These results agree with HRTEM images depicted in insets of Figures 2a-c, where we can also identify some of these planes. At this point, we deduced that organic ligands do not induce changes in the crystal structure of the PQDs after the embedding process.

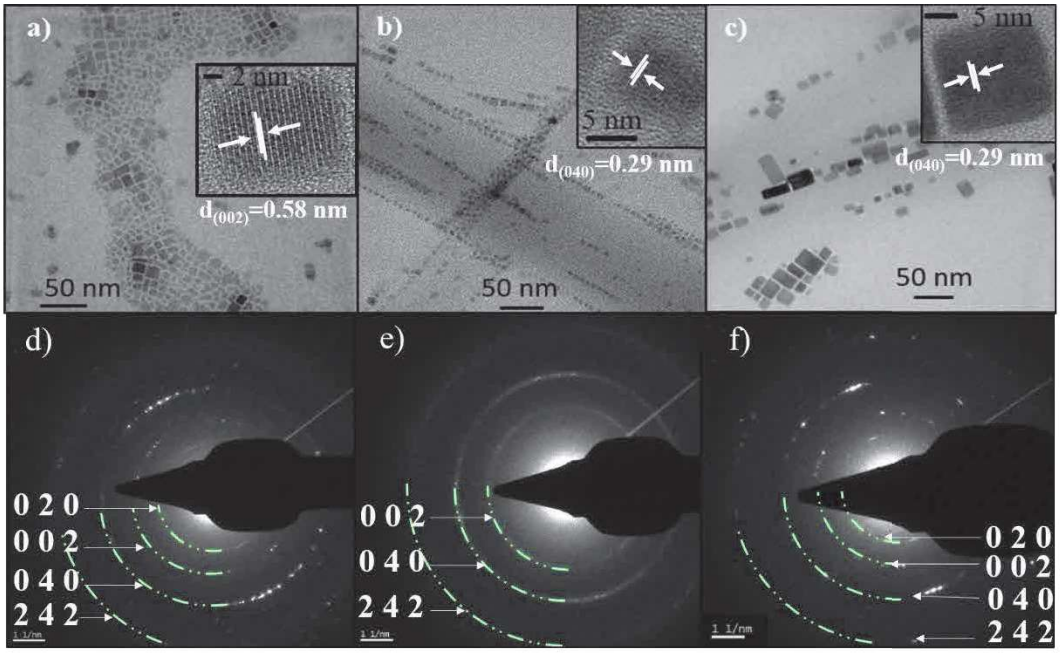

Figure 2. a) and d) TEM image and SAED patterns of the $CsPbBr_3$ PQDs solution. b) and e) TEM image and SAED patterns of the Hx-PQDs gel. c) and f) TEM image and SAED patterns of the Chx-PQDs gel. Insets in the TEM images are corresponding HRTEM images.

Fourier transformed infrared spectroscopy (FTIR) was employed to obtain information about the ligands covering the PQDs surface. In **Figure 3a**, three samples are shown: $CsPbBr_3$ PQDs

solution, Hx gel and Hx-PQDs. Then, a comparison between Chx and Chx-PQDs samples is also shown in **Figure 3b**. From $CsPbBr_3$ PQDs solution, the signals in the range of 2852-2956 cm^{-1} and 1465 cm^{-1} correspond to the presence of OA and OLEA covering the PQDs surface. These bands are associated to C-H stretching and C-H bending, respectively. A broad band starting at 3300 cm^{-1} is associated to O-H stretching, while a band at 1715 cm^{-1} is ascribed to C=O stretching of the carboxylic acid. Moreover, bands observed at 1534 and 1406 cm^{-1} are associated to the O-C-O stretching.[32,33] **Figure S5** shows the typical FTIR of OA and OLEA, where their corresponding peaks match with those of the PQDs. These results corroborate the assignment of the bands above. Then, in Hx gel spectrum, the most significant bands appear at 3283 cm^{-1} from N-H stretching, 1697 cm^{-1} from C=O (carboxylic group) and from the amides at 1632 and 1540 cm^{-1}. [9,32] In Hx-PQDs spectrum, the peaks match with the ones in the reference sample with slight variations in the position. Comparing these three samples, a decrease in the relative intensity of the assigned band at 1697 cm^{-1} in Hx-PQDs spectrum is observed, which may suggest that there is an interaction that reduces the C=O vibrational mode. However, by comparing the FTIR spectra of Chx and Chx-PQDs samples, there is no significant variation in the relative intensity of the bands.[9] At this stage, we deduce that Hx shows a high influence on the surface properties of $CsPbBr_3$ PQDs compared with Chx organic ligand, which does not seem to suffer any alteration after interacting with the perovskite colloidal solution. This observation can corroborate that Chx is more prone to self-associate due to the preorganization of its molecular structure, whereas Hx, less preorganized, is more available for the interaction at the surface of the PQDs.

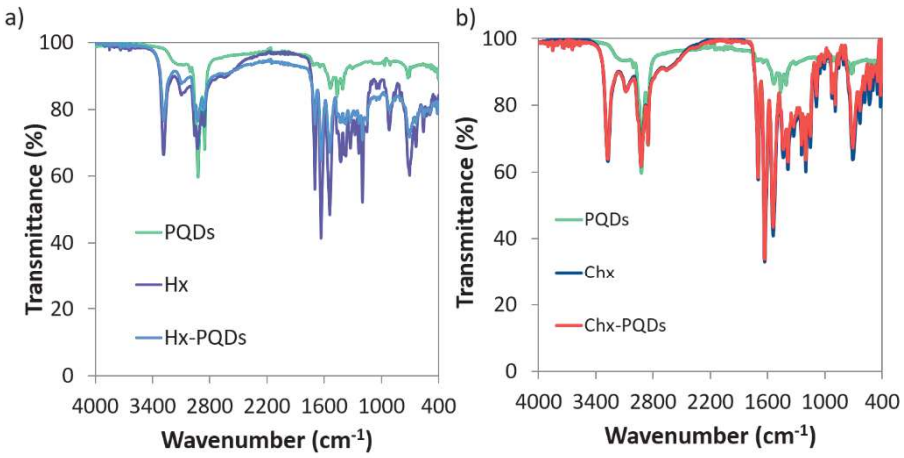

Figure 3. a) FTIR spectra of $CsPbBr_3$ PQDs in solution (green), Hx gel matrix (purple) and Hx with embedded PQDs (blue). b) FTIR spectra of $CsPbBr_3$ PQDs in solution (green), Chx gel matrix (dark blue) and Chx with embedded PQDs (red).

The stability of $CsPbBr_3$ PQDs has been also studied under ambient conditions in presence of the organogelators. By measuring the PLQY of these materials, $CsPbBr_3$ PQDs colloidal solution in absence of the matrices displays a value around 62% after one purification. By adding the gelators and forming the gel, Hx-PQDs sample shows a higher improvement of PLQY with values arriving to 95%, while Chx-QDs one was 70% (**Figure 4a**). After 6 months, Hx-PQDs and Chx-PQDs have retained the PLQY around 76% and 77% from their initial value, respectively. Simultaneously, the emission peak position of Hx-PQDs shows a slight blueshift along the time, starting at 490 nm and moving to 480 nm. Unlike the ligand exchange process, where it was described the substitution of OA and OLEA with another capping ligands,[20] we associate this phenomenon to the gradual ligand passivation provided by Hx matrix, since some OA and OLEA ligands are removed from PQDs surface after purification step. Thus, more active sites are available for Hx to interact with the PQDs surface. Nevertheless, PL does not present any shift after some days, indicating that the ligand passivation was completed. For the case of Chx-PQDs, the emission peak position remains around 517 nm, suggesting that Chx

matrix could not compensate the loss of ligands from purified PQDs. Then, by considering that the PLQY of the $CsPbBr_3$ PQDs was increased in presence of Hx, we presume that this aminoacid derivative maximizes the reduction of surface defects from PQDs, mitigating the non-radiative recombination trapping. To corroborate this hypothesis, we performed time-resolved PL (TRPL) measurements (**Figure 4c**) for the samples after 6 months, where PL parameters such as lifetime (τ_{avg}), radiative and non-radiative carrier recombination constants (k_r and k_{nr}, respectively) were estimated (**Table S3**). Although it is true that unmodified PQDs, Hx-PQDs and Chx-PQDs show similar k_r, Hx-PQDs exhibits the longest lifetime, and the lowest k_{nr} and k_{nr}/k_r. Accordingly, we deduce that Hx provides a better surface passivation than Chx matrix, hampering the non-radiative recombination mechanism and promoting the radiative channel for electron relaxation. This fact explains the PLQY improvement up to near-unity and long-term stability of Hx-PQDs. In the case of Chx-PQDs, the highest k_{nr} is a clear indication that the non-radiative recombination mechanism is facilitated, which could be associated to intraband gap energy levels formed by PQDs agglomeration.

According to the above-mentioned results, we suggest that Hx can promote a better coverage of PQDs surface due to its linear hexyl chain radical with a low grade of steric hindrance. In contrast, in the case of Chx, the cyclohexyl radical can provide a strong steric hindrance, restraining the ligand passivation. Therefore, we concluded that Hx can be used as an efficient surface ligand passivator during the post-synthetic treatment of $CsPbBr_3$ PQDs, which increase the quality of the materials and their stability.

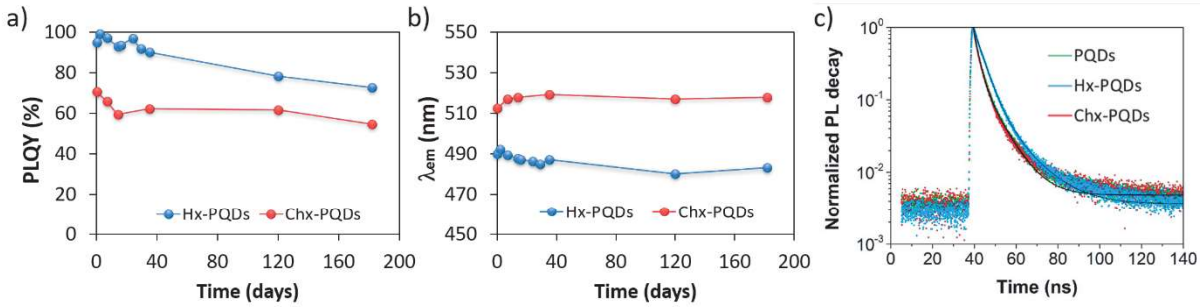

Figure 4. Evolution of a) PLQY and b) the emission wavelength of both gel matrixes: Hx (blue) and Chx (red). c) TRPL of PQDs (green), Hx-PQDs (blue) and Chx-PQDs (red) recorded 6 months after synthesis.

3. Summary and Conclusions

In this study, two different organogels with embedded $CsPbBr_3$ perovskite quantum dots, Hx-PQDs and Chx-PQDs, have been successfully prepared. The difference in the structure of these organogelators shows an effect on the PQDs, varying the emission from green to blue in the case of Hx gel. In addition to this effect, the PLQY increases, which points to an interaction between the organogels and the surface of the PQDs as shows the FTIR spectra. In the case of Hx, this short-chain amino acid derivative can slightly decrease the particle size, promoting (1) high PQDs monodispersity and blueshift of PL, and (2) efficient passivation of the PQDs surface. This fact hinders the non-radiative carrier recombination pathway to facilitate the radiative channel. Hence, a near-unity PLQY can be achieved with a long-term stability. For Chx, the cyclohexyl radical, due to self-assembly and steric hindrance, inhibits the ligand passivation and generates a lower improvement in the photophysical features of the PQDs. Although original green emission is slightly redshifted due to PQD size increase.

Accordingly, the use of organogelators based on linear amino acids is a potential post-synthetic approach to improve the quality of PQDs. It is important to highlight that the blueshift is observed even for a low concentration of organogelators which can be widely useful for optoelectronics. Consequently, this communication points to a very interesting research line on the tunability of PQDs light emission by the use of external additives.

4. Experimental Section

Synthesis of $CsPbBr_3$ PQDs: $CsPbBr_3$ PQDs synthesis and purification were based on previously reported methods.[3,34] For the Cs-oleate solution, 0.618 g Cs_2CO_3 (Sigma-Aldrich, 99.9 %), 1.9 mL OA (Sigma Aldrich, 90 %) and 30 mL of 1-octadecene (ODE, Sigma-Aldrich, 90 %) were kept under continuous stirring under vacuum at 80 ºC and 120 °C 30 min each. Then, the solution was heated at 140 °C in nitrogen atmosphere until the Cs_2CO_3 was completely dissolved and, after that, it was kept at 120 °C.

1.0 g $PbBr_2$ (ABCR, 99.999 %) in 50 mL ODE was heated at 120 ºC under continuous stirring and kept 1 h at this temperature under vacuum. Then, under N_2, 5 mL OA and 5 mL OLEA (Sigma-Aldrich, 98 %) were added to the flask and the solution was heated to 175 °C, injecting quickly 4 mL Cs-oleate solution and after 5 s the reaction was quenched by cooling down the reaction in an ice bath.

$CsPbBr_3$ PQDs were isolated and purified by adding 60 mL of methyl acetate and centrifuging the mixture at 4700 rpm 5 min. The precipitated PQDs where dispersed in hexane (Honeywell, 99.7%). To obtain the desired concentration, the PQDs solution was dried and re-dispersed in toluene for a final concentration 50 mg mL^{-1}.

Preparation of the gels: Syntheses of Hx and Chx were based on a previous report.[25] The different gelators were weighed to obtain a 2.5 mg mL^{-1} solution in toluene for Hx and 2.0 mg mL^{-1} for Chx. To form the gel matrix, they were heated with an air gun and let it cool down. When they were completely formed, the perovskite QDs were added to obtain a final concentration of 1 mg mL^{-1} and the gels were heated and cooled again.

Characterization: PL and PLQY measurements were carried out using an absolute quantum yield spectrometer (C9920-02, Hamamatsu) with an integral sphere, fixing the absorbance values in a range around 0.3-0.6, using a Xe lamp (150 W) as light source. Samples were excited at 350 nm. Time-resolved PL measurements were performed through photoluminescence spectrophotometer (Fluorolog 3-11, Horiba) at 405 nm pulsed laser (1 MHz frequency, NanoLED-405L, <100 ps of pulse width). Transmission Electron Microscopy (TEM) measurements were carried out in a field emission gun TECNAI G^2 F20 microscope operated at 200 kV. UV-visible absorption spectra were measured by a PerkinElmer LAMBDA 1050+ UV/Vis/NIR spectrophotometer. FTIR spectroscopy was measured using a FTIR spectrometer FT/IR-6200 (Jasco) in ATR using a diamond glass.

Supporting Information

Supporting Information is available from the Wiley Online Library or from the author.

Acknowledgements

M.V.-P. A. G.-R. and I.M.-S. acknowledge the support of the European Research Council (ERC) via Consolidator Grant (724424 - No-LIMIT) and Generalitat Valenciana via Prometeo Grant Q-Devices (Prometeo/2018/098). M. V-P. acknowledges Universitat Jaume I for the support through FPI Fellowship Program (PREDOC/2017/40). F.G. and J. F. M. acknowledge the support of Spanish Ministerio de Ciencia, Innovación y Universidades (RTI2018-101675-B-I00). S.A. and V.M.-S. acknowledge the support of the EU (FEDER) and MINECO under project TEC2017-85912-C2-2. We acknowledge SCIC from UJI for help with FTIR

characterization. Authors thank Dr. Samrat Das Adhikari for his useful comments about the manuscript.

Received: ((will be filled in by the editorial staff))
Revised: ((will be filled in by the editorial staff))
Published online: ((will be filled in by the editorial staff))

References

[1] B. J. Bohn, Y. Tong, M. Gramlich, M. L. Lai, M. Döblinger, K. Wang, R. L. Z. Hoye, P. Müller-Buschbaum, S. D. Stranks, A. S. Urban, L. Polavarapu, J. Feldmann, *Nano Lett.* **2018**, *18*, 5231.

[2] Q. Van Le, K. Hong, H. W. Jang, S. Y. Kim, *Adv. Electron. Mater.* **2018**, *4*, 1800335.

[3] L. Protesescu, S. Yakunin, M. I. Bodnarchuk, F. Krieg, R. Caputo, C. H. Hendon, R. X. Yang, A. Walsh, M. V Kovalenko, *Nano Lett.* **2015**, *15*, 3692.

[4] A. Dutta, S. K. Dutta, S. Das Adhikari, N. Pradhan, *ACS Energy Lett.* **2018**, *3*, 329.

[5] S. Huang, M. Guo, J. Tan, Y. Geng, J. Wu, Y. Tang, C. Su, C. C. Lin, Y. Liang, *ACS Appl. Mater. Interfaces* **2018**, *10*, 39056.

[6] C.-Y. Huang, C. Zou, C. Mao, K. L. Corp, Y.-C. Yao, Y.-J. Lee, C. W. Schlenker, A. K. Y. Jen, L. Y. Lin, *ACS Photonics* **2017**, *4*, 2281.

[7] Y. Wang, X. Li, J. Song, L. Xiao, H. Zeng, H. Sun, *Adv. Mater.* **2015**, *27*, 7101.

[8] F. Zhou, Z. Li, W. Lan, Q. Wang, L. Ding, Z. Jin, *Small Methods* **2020**, *n/a*, 2000506.

[9] M. Fang, S. Huang, D. Li, C. Jiang, P. Tian, H. Lin, C. Luo, W. Yu, H. Peng, *Nanophotonics* **2018**, *7*, 1949.

[10] J. Xing, Y. Zhao, M. Askerka, L. N. Quan, X. Gong, W. Zhao, J. Zhao, H. Tan, G. Long, L. Gao, Z. Yang, O. Voznyy, J. Tang, Z.-H. Lu, Q. Xiong, E. H. Sargent, *Nat. Commun.* **2018**, *9*, 3541.

[11] N. Mondal, A. De, A. Samanta, *ACS Energy Lett.* **2019**, *4*, 32.

[12] N. K. Kumawat, X.-K. Liu, D. Kabra, F. Gao, *Nanoscale* **2019**, *11*, 2109.

[13] A. Dutta, R. K. Behera, P. Pal, S. Baitalik, N. Pradhan, *Angew. Chemie Int. Ed.* **2019**, *58*, 5552.

[14] P. D. Wadhavane, R. E. Galian, M. A. Izquierdo, J. Aguilera-Sigalat, F. Galindo, L. Schmidt, M. I. Burguete, J. Pérez-Prieto, S. V Luis, *J. Am. Chem. Soc.* **2012**, *134*, 20554.

[15] W. J. Peveler, J. C. Bear, P. Southern, I. P. Parkin, *Chem. Commun.* **2014**, *50*, 14418.

[16] J.-M. Park, J. Park, Y.-H. Kim, H. Zhou, Y. Lee, S. H. Jo, J. Ma, T.-W. Lee, J.-Y. Sun, *Nat. Commun.* **2020**, *11*, 4638.

[17] M. Yamauchi, Y. Fujiwara, S. Masuo, *ACS Omega* **2020**, *5*, 14370.

[18] R. Nadler, J. F. Sanz, *J. Phys. Chem. A* **2015**, *119*, 1218.

[19] J. Amaya Suárez, J. J. Plata, A. M. Márquez, J. Fernández Sanz, *J. Phys. Chem. A* **2017**, *121*, 7290.

[20] S. R, H. V Vishaka, K. J, R. G. Balakrishna, *ACS Appl. Nano Mater.* **2020**, *3*, 6089.

[21] C. Sun, Y. Zhang, C. Ruan, C. Yin, X. Wang, Y. Wang, W. W. Yu, *Adv. Mater.* **2016**, *28*, 10088.

[22] Y. Cai, Y. Li, L. Wang, R.-J. Xie, *Adv. Opt. Mater.* **2019**, *7*, 1901075.

[23] Y. Wei, H. Xiao, Z. Xie, S. Liang, S. Liang, X. Cai, S. Huang, A. A. Al Kheraif, H. S. Jang, Z. Cheng, J. Lin, *Adv. Opt. Mater.* **2018**, *6*, 1701343.

[24] D. H. Park, J. S. Han, W. Kim, H. S. Jang, *Dye. Pigment.* **2018**, *149*, 246.

[25] C. A. Angulo-Pachón, C. Gascó-Catalán, J. J. Ojeda-Flores, J. F. Miravet, *ChemPhysChem* **2016**, *17*, 2008.

[26] J. B. Hoffman, G. Zaiats, I. Wappes, P. V Kamat, *Chem. Mater.* **2017**, *29*, 9767.

[27] Y. De Smet, L. Deriemaeker, R. Finsy, *Langmuir* **1997**, *13*, 6884.

[28] F. Bertolotti, G. Nedelcu, A. Vivani, A. Cervellino, N. Masciocchi, A. Guagliardi, M. V Kovalenko, *ACS Nano* **2019**, *13*, 14294.

[29] P. Cottingham, R. L. Brutchey, *Chem. Commun.* **2016**, *52*, 5246.

[30] M. C. Brennan, M. Kuno, S. Rouvimov, *Inorg. Chem.* **2019**, *58*, 1555.

[31] P. Cottingham, R. L. Brutchey, *Chem. Mater.* **2018**, *30*, 6711.

[32] J. Pan, L. N. Quan, Y. Zhao, W. Peng, B. Murali, S. P. Sarmah, M. Yuan, L. Sinatra, N. M. Alyami, J. Liu, E. Yassitepe, Z. Yang, O. Voznyy, R. Comin, M. N. Hedhili, O. F. Mohammed, Z. H. Lu, D. H. Kim, E. H. Sargent, O. M. Bakr, *Adv. Mater.* **2016**, *28*, 8718.

[33] L. C. Cass, M. Malicki, E. A. Weiss, *Anal. Chem.* **2013**, *85*, 6974.

[34] A. Swarnkar, A. R. Marshall, E. M. Sanehira, B. D. Chernomordik, D. T. Moore, J. A. Christians, T. Chakrabarti, J. M. Luther, *Science (80-.).* **2016**, *354*, 92 LP.

[35] V. K. Ravi, R. A. Scheidt, A. Nag, M. Kuno, P. V Kamat, *ACS Energy Lett.* **2018**, *3*, 1049.

Marta Vallés-Pelarda, Andrés F. Gualdrón-Reyes, Carles Felip-León, César A. Angulo-Pachón, Said Agouram, Vicente Muñoz-Sanjosé, Juan F. Miravet*, Francisco Galindo*, Iván Mora-Seró*

High optical performance of cyan-emissive $CsPbBr_3$ perovskite quantum dots embedded in molecular organogels

ToC figure

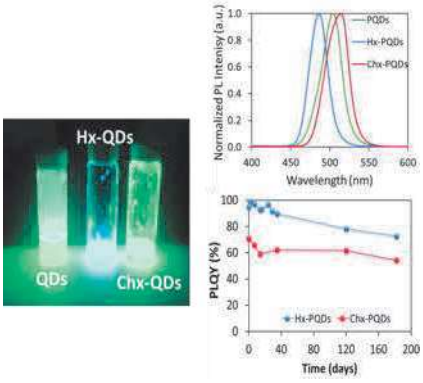

$CsPbBr_3$ perovskite quantum dots are embedded in two different organogels, Hx and Chx. Both short-chain capping ligands improve the photophysical properties of PQDs, being more significative by using the hexyl-radical aminoacid derivative. In this case, near-unity PLQY with blue emission and long-term stability is achieved, considering this post-synthetic treatment attractive for enhancing the quality of blue-emissive PQDs.